Chemical Physics Letters 537 (2012) 33–37

Contents lists available at SciVerse ScienceDirect

Chemical Physics Letters

journal homepage: www.elsevier.com/locate/cplett

Why mixtures of hydrazine and dinitrogen tetroxide are hypergolic?

Ke-Yu Lai [a], Rongshun Zhu [b], M.C. Lin [a,b,*]

[a] Center for Interdisciplinary Molecular Science, National Chiao Tung University, Hsinchu 300, Taiwan
[b] Department of Chemistry, Emory University, Atlanta, GA 30322, USA

ARTICLE INFO

Article history:
Received 24 February 2012
In final form 3 April 2012
Available online 14 April 2012

ABSTRACT

The reactions of N_2H_4 with N_2O_4 isomers have been investigated at the G2M(CC3)//B3LYP/6-311++G(3df,2p) level. The results show that the reactions of N_2H_4 with sym-N_2O_4 (D_{2h}), cis-$ONONO_2$ (C_s), and NO_2 have to overcome 14.2, 10.6, and 7.6 kcal/mol barriers, respectively. However, N_2H_4 can react spontaneously with trans-$ONONO_2$ (C_s) and cis-$ONONO_2$ (C_1) to produce $HONO_2$ + $H_2NN(H)NO$ with the near gas-kinetic rate constant, 4×10^{-10} cm^3 $molecule^{-1}$ s^{-1} above 250 K. The $H_2NN(H)NO$ thus formed can rapidly fragment to give reactive N_2H_3 radical with rate constant > 1×10^7 s^{-1} at 1000 K, which is fast enough to initiate the hypergolic chain reactions with NO_2 and N_2O_4.

© 2012 Elsevier B.V. All rights reserved.

1. Introduction

The hydrazine (N_2H_4) and dinitrogen tetroxide (N_2O_4) reaction system is widely used as liquid propellants of the spacecrafts and the rockets [1–3]. The liquid fuel (N_2H_4) and the liquid oxidizer (N_2O_4) have been stored separately in isolated containers initially at 100–325 psia and 20–26 °C conditions [4–6]; the reaction ignites spontaneously producing a large amount of flame and gases when the two high-pressure reagents are ejected and mixed in the engine. There were some NASA reports in 1960's [4,7–10] which discussed the applications and the phenomenon of the spontaneous reaction of N_2H_4 and N_2O_4; most of the previous studies focused on the engine design or mixing ratios of the two reactants. In 1965, Weiss [7] studied this reaction by infrared spectroscopy, but not enough information was provided to explain the mechanism of the hypergolic process due to the complexity of the reaction. To date, the mechanism of the hypergolic process is still unsolved, despite the great practical importance of this propellant system. Structurally, the N_2O_4 molecule is known to have different conformers, the commonly known sym-N_2O_4 with D_{2h} symmetry and asymmetric $ONONO_2$ with cis- and trans-structures. The concentration of $ONONO_2$ isomers has been estimated to be in the range of 0.05% of N_2O_4 [11]. The major goal of this Letter is to elucidate how the hypergolic reaction occurs and what are the roles of symmetric and asymmetric isomers of N_2O_4 in the hypergolic *initiation* reaction? Our computational strategy is to search for the elementary reactions with high exothermicities and low activation barriers which allow the chemistry to take off hypergolically.

2. Computational methods

All ab initio calculations were performed by using the GAUSSIAN 03 suite of programs [12]. The equilibrium geometries, including reactants, intermediates (IMs), transition states (TSs), and products, were optimized by using the density functional theory (DFT) with the hybrid B3LYP functionals [13–16] in conjunction with the 6-311++G(3df,2p) basis set with polarized and diffuse functions. The zero-point energy (ZPE) and the harmonic vibrational frequency were also determined by the same method. All stationary points are identified for local minima (without any imaginary frequency) and transition states (each with one imaginary frequency). The intrinsic reaction coordinate (IRC) calculations [17] were used to confirm that transition states connect between designed intermediates. More accurate single-point energies were refined by the G2M (CC3) method [18].

Rate constants for the low-energy channels and product fragmentation have been predicted by the Rice–Ramsperger–Kassel–Marcus (RRKM) theory implemented in the Variflex code [19]. The minimum energy paths (MEPs) representing the barrierless association of N_2H_4 with trans-$ONONO_2$ (C_s) and cis-$ONONO_2$ (C_1) and direct dissociation of $H_2NN(H)NO$ are obtained by calculating the potential energy curves along the reaction coordinates (the N–N bonds in the complexes IM1c and IM1d see Figure 2 and in the product $H_2NN(H)NO$ see Figure S2), where the N–N bond lengths are stretched from the equilibrium values of 1.874, 2.033, and 1.331 Å to 5.072, 4.533, and 5.131 Å with an interval step size of 0.2 Å, other geometric parameters are fully optimized. The dissociation curve can be fitted to the Morse potential function $E(R) = D_e [1 - \exp(-\beta(R - R_e))]^2$, which is employed to approximate the MEP path for the variational transition state in the rate calculation. In the above equation, R is the reaction coordinate (i.e., the distance between the two bonding atoms; R(N–N)), D_e is the bond energy

* Corresponding author at: Department of Chemistry, Emory University, Atlanta, GA 30322, USA.
E-mail address: chemmcl@emory.edu (M.C. Lin).

0009-2614/$ - see front matter © 2012 Elsevier B.V. All rights reserved.
http://dx.doi.org/10.1016/j.cplett.2012.04.015

excluding zero-point energy and R_e is the equilibrium value of R (1.874, 2.033, and 1.331 Å). The computed potential energies can be fitted reasonably to the Morse potential function with the parameter β = 1.886, 2.220, and 1.265 $Å^{-1}$, respectively. The calculated dissociation curves are shown in Figure S1 of Supplementary information. The numbers of states for the tight transition states are evaluated according to the rigid-rotor harmonic-oscillator assumption. For those paths involving hydrogen atom transfers, Eckart tunneling effects [20,21] were taken into account in the rate constant calculation.

3. Results and discussion

Besides sym-N_2O_4, many experimental studies [11,22–33] revealed the existence of asymmetric N_2O_4 isomers but their geometries are not well characterized. Previous ab initio calculations predicted the possible geometries of trans-$ONONO_2$ (C_s-symmetry) [34,35], cis-$ONONO_2$ (C_s-symmetry) [36], and cis-$ONONO_2$ (C_1-symmetry) [37]; therefore, we have also considered these isomeric reactions with N_2H_4. In addition, since sym-N_2O_4 can easily dissociate to two NO_2 with only 12.7 kcal/mol dissociation energy [38], the mechanism of NO_2 interacting with N_2H_4 is also calculated in this Letter. The geometries of all reactants and products including selective bond lengths, angles, and Mulliken charges are shown in Figure S2 of Supplementary information.

3.1. $N_2H_4 + NO_2$ (C_{2v}) reaction

The major path of the potential energy profile for the $N_2H_4 + NO_2$ reaction is shown in Figure 1a; the detailed potential energy profile and the geometries for the key intermediates and transitions states are displayed in Figures S3–S4 of Supplementary information. For the most favorite channel (Figure 1a), the reaction of N_2H_4 with NO_2 forms a loose complex (IM1a) with 2.5 kcal/mol association energy, which can readily transform to IM2a via TS1a with only 5.0 kcal/mol barrier; the hydrogen abstraction reaction from IM2a via TS2a needs to overcome 4.2 kcal/mol barrier to produce a product side complex IM3a which can further dissociate to the final products, N_2H_3 + cis-HONO with slight endothermicity (3.4 kcal/mol). From the PES in Figure 1a one can see that TS2a is the rate-controlling point, lying 7.6 kcal/mol above the reactants. The maximum rate constant for this lowest-energy-barrier path in the $N_2H_4 + NO_2$ reaction, can be represented as $k_a = 5.36 \times 10^{-24} T^{3.56} \exp(384/T)$ cm^3 $molecule^{-1}$ s^{-1} from 250 to 2500 K, with a relatively low value $k_a = 1.06 \times 10^{-14}$ cm^3 $molecule^{-1}$ s^{-1} at 1000 K.

3.2. $N_2H_4 + N_2O_4$ (D_{2h}) reaction

The major path for this reaction is shown in Figure 1b. The initial complex, IM1b with 7.0 kcal/mol association energy, can transform to a more stable IM2b of the products (trans-HONO and $H_2NN(H)NO_2$), via a five-member ring TS1b lying above the reactants by 14.2 kcal/mol, which is 3.9 kcal/mol higher than that of the analogous N–H abstraction by NO_2. For other reaction paths, the energy barriers are higher than 20 kcal/mol; their potential energy profiles and details of geometries are shown in Figure S5–S6 of Supplementary information. The rate constant of the lowest-energy-barrier reaction path (Figure 1b) can be represented as: $k_b = 2.30 \times 10^{-22} T^{2.62} \exp(-6598/T)$ cm^3 $molecule^{-1}$ sec^{-1} from 250 to 2500 K; the reaction is too slow to help the chain initiation process.

3.3. $N_2H_4 + ONONO_2$ reactions

The trans-$ONONO_2$ (C_s) and non-planar cis-$ONONO_2$ (C_1) isomers have similar structures with the ON–ONO_2 bond length of 1.621 and 1.685 Å, respectively. Experimental studies [26–30] indicate that the autoionization of these isomers forming ionic nitrosonium nitrate ($[ON^+][NO_3^-]$) occurs. In the N_2H_4 + trans-$ONONO_2$ reaction, the interaction between the two reactants forms a complex IM1c with 10.1 kcal/mol association energy, in which the ON–ONO_2 bond is lengthened to 2.286 Å, suggesting that N_2H_4 may induce the ionization of ON–ONO_2 to $[ON^+][NO_3^-]$; based on the Mulliken analysis, the charges on ON and NO_3 are 0.146e and −0.768e, respectively. The NO_3 group can abstract one of the H atoms in N_2H_4 via a six-member ring TS1c with a negligible barrier (0.2 kcal/mol at the B3LYP level) to produce a product-side complex $HONO_2$–$H_2NN(H)NO$ with a 25.8 kcal/mol exothermicity. The lowest energy channel of the N_2H_4 + trans-$ONONO_2$ (C_s) reaction is shown in Figure 2a, and the details of geometries are presented in Figure S7. It needs to be mentioned that at the B3LYP level, energy of TS1c is slightly higher than that of IM1c by 0.2 kcal/mol; however, at the G2M-CC3 level, TS1c is lower than IM1c by 2.7 kcal/mol. IRC result shows that IM1c can readily transform to the IM2c with a sharp slope, implying that IM1c is most likely to be metastable or unstable. Similar phenomenon also appears in IM1d and TS1d. The final products, $HONO_2$ and $H_2NN(H)NO$ have 21.1 kcal/mol exothermicity. Due to the low energy of TS1c (lying below the reactants by 12.8 kcal/mol) and the smaller decomposition energy (4.6 kcal/mol) of IM2c, one can expect that the interaction of N_2H_4 with trans-$ONONO_2$ forms IM1c which readily produces final products; therefore, the collisional deactivation of IM2c can be reasonably ignored. The rate constant for this process has a negligible temperature dependence in the range of 250–2500 K and can be effectively expressed by $k_c = 4.3 \pm 0.5 \times 10^{-10}$ cm^3 $molecule^{-1}$ sec^{-1}.

Due to the similar geometries and charge distributions of trans-$ONONO_2$ (C_s) and cis-$ONONO_2$ (C_1), the mechanism for N_2H_4 + cis-$ONONO_2$ (C_1) is expected to be similar to that of N_2H_4 + trans-$ONONO_2$ presented above. The lowest energy path is shown in Figure 2b, and the details of geometries are presented in Figure S8. The direct hydrogen abstraction reaction via TS1d (with a four-member ring structure) also produces the $H_2NN(H)NO$ and HNO_3. The electronic energy of $TS1_d$ computed at B3LYP is 1.04 kcal/mol higher than IM1d; however, at the G2M (CC3) level, the energy of TS1d is lower than that of IM1d by 2.8 kcal/mol, again reflecting the negligibly small TS barrier for the ionic transformation. It should be mentioned that at the G2M(CC3) level, the T1 diagnostics values in the CCSD(T) method are both 0.019 and 0.019 for the low-energy transition states (TS1c and T1d), which are lower than the proposed maximum value of 0.02 [39,40]. In the high-energy TS1a, TS2a and TS1b, the T1 values, 0.020, 0.028, 0.025, are close to the proposed maximum value of 0.02*; these higher energy TS's are not important to the hypergolic initiation process.* Other species in this system don't have spin contaminated problem. Similar to the above reaction, the reaction of N_2H_4 + cis-$ONONO_2$ (C_1) producing the same pair of products is very fast and the rate constant can be effectively expressed by $k_d = 3.5 \pm 0.5 \times 10^{-10}$ cm^3 $molecule^{-1}$ sec^{-1} in the temperature range of 250–2500 K with a negligible temperature dependence.

Interestingly, the geometry and charge distribution of cis-$ONONO_2$ (C_s) are noticeably different from those of trans-$ONONO_2$ and cis-$ONONO_2$ (C_1) isomers (see Figure S2); the reaction of N_2H_4 with cis-$ONONO_2$ (C_s) has to overcome as much as 10.6 kcal/mol of barrier to produce HONO + $H_2NN(H)NO_2$. The potential energy profile and the geometric parameters are shown in Figure S9. Apparently, this reaction channel cannot compete with the above two reactions, its rate constant was not calculated.

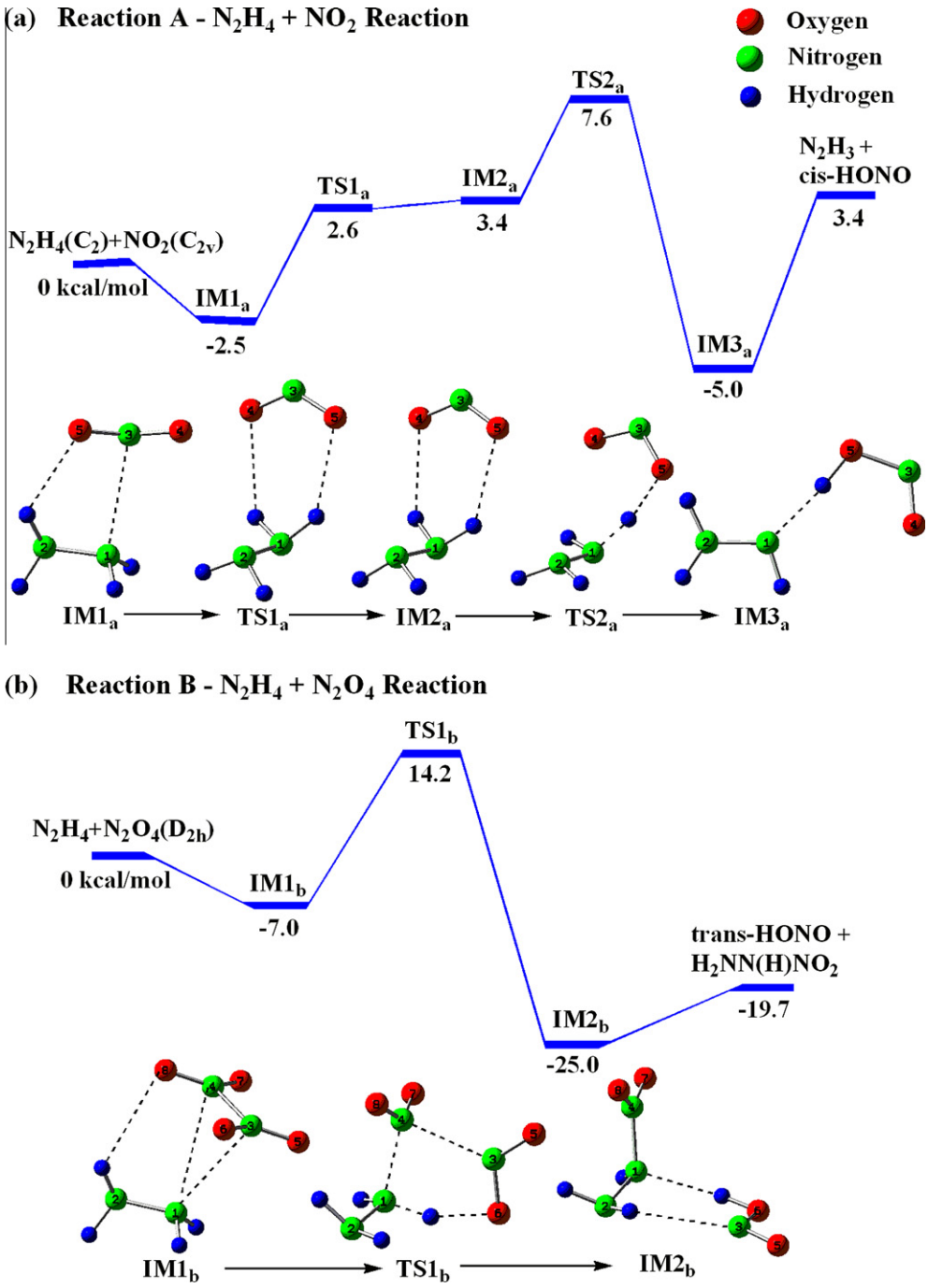

Figure 1. The major path of potential energy profile and schematic geometry of species for (a) N_2H_4 + NO_2 (C_{2v}) and (b) N_2H_4 + N_2O_4 (D_{2h}). Relative energies (kcal/mol) are calculated with G2M-CC3 based on B3LYP geometries.

3.4. Unimolecuar decomposition of $H_2NN(H)NO$

The exothermic reaction product, $H_2NN(H)NO$, from the reactions of N_2H_4 with trans-$ONONO_2$ and cis-$ONONO_2$ (C_1), was predicted to decompose to N_2H_3 and NO radicals readily without an intrinsic barrier. Calculated rate constant for the dissociation of $H_2NN(H)NO \rightarrow N_2H_3 + NO$, with the energies predicted by the direct CCSD(T)/6-311++G(3df,2p) calculation can be expressed as $k_{dis} = 6.24 \times 10^{15}\, T^{-0.15}\, \exp(-17\,920/T)\ sec^{-1}$ from 250 to 1500 K with $k_{dis} = 0.65$ and $3.74 \times 10^7\ s^{-1}$ at 500 and 1000 K, respectively. The reactive N_2H_3 radical formed by the decomposition can easily initiate chain reactions with NO_2 and N_2O_4 present in large concentrations. For example, the $N_2H_3 + NO_2$ reaction is expected to produce $N_2H_3O + NO$ [41] and $H_2NN(H)O + OH$ among other fragile products. N_2H_3O can readily produce $H_2NNO + H$ and $N_2H_2 + OH$; all are potential chain propagators.

4. Conclusion

The reactions of N_2H_4 with trans-$ONONO_2$ (C_s) and cis-$ONONO_2$ (C_1) have been shown to play a very crucial role in the auto-ignition

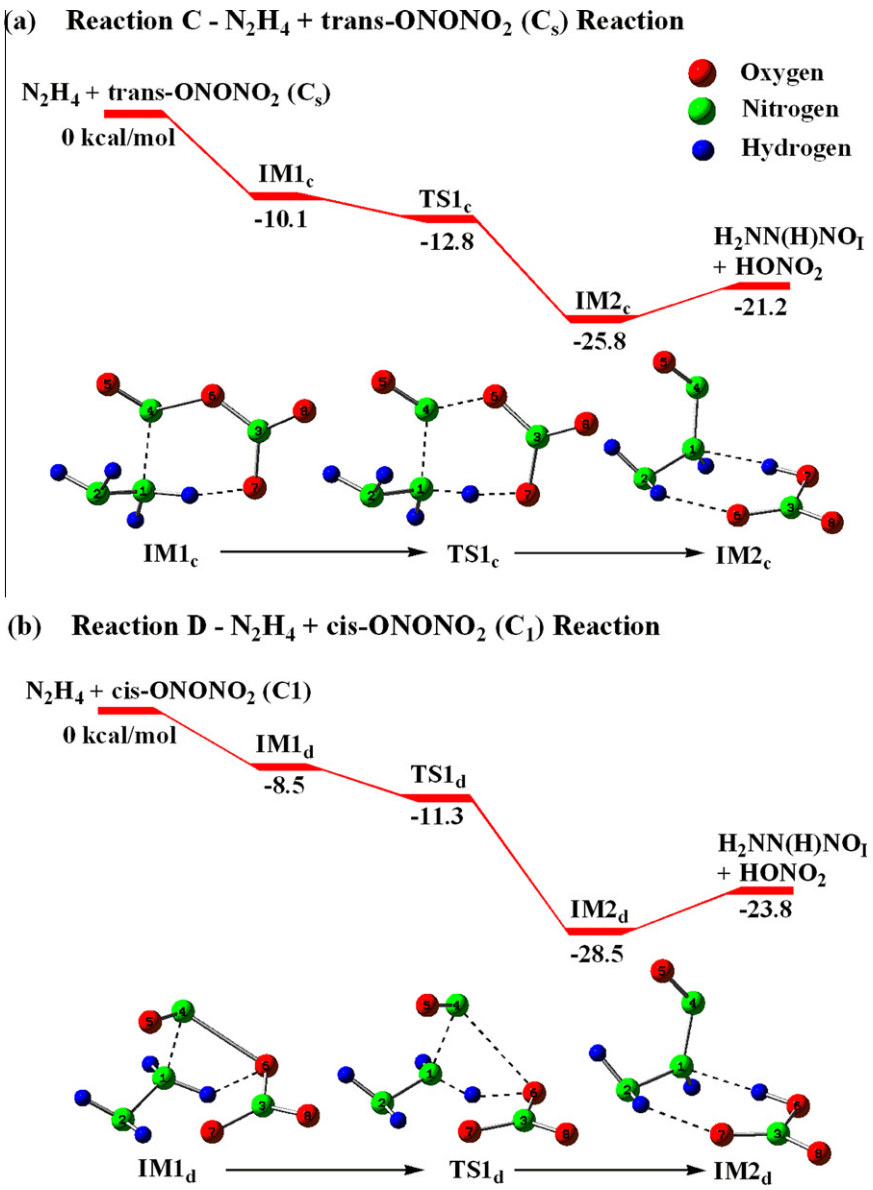

Figure 2. The major path of potential energy profile and schematic geometry of species for (a) N_2H_4 + trans-$ONONO_2$ (C_s) and (b) N_2H_4 + cis-$ONONO_2$ (C_1). Relative energies (kcal/mol) are calculated with G2M-CC3 based on B3LYP geometries.

reaction of mixtures of hydrazine and dinitrogen tetraoxide. Calculated results show that N_2H_4 can induce the ionization of trans-$ONONO_2$ (C_s) and cis-$ONONO_2$ (C_1) to $[ON^+][ONO_2^-]$, which readily undergoes metathetical reaction to produce exothermic products, $HONO_2$ and $H_2NN(H)NO$; the latter can further decompose into N_2H_3 and NO radicals to initiate chain reactions by fast exothermic reactions, such as $N_2H_3 + NO_2$ and $N_2H_3 + N_2O_4$, giving H and OH chain carriers with the release of a large amount of energy. Similar reactions of substituted hydrazines such as CH_3NHNH_2 and $(CH_3)_2NNH_2$ are expected to react readily with the isomers of $ONONO_2$ to produce H and OH chain carriers for the known hypergolic reactions. The concentration of $ONONO_2$ isomers has been estimated to be in the range of 0.05% of N_2O_4 [11] which is very close to our computed value, 0.058%, based on the calculated equilibrium constant of N_2O_4 and $ONONO_2$ using the energies and geometric parameters predicted in this Letter. The variation of $ONONO_2$ concentration with temperature can be expressed as $[ONONO_2] = 12.46 \times \exp(-2971/T)\,[N_2O_4]$ in the range of 200–800 K. The results suggest that the hypergolic chain initiation process as predicted can occur with a very high rate because of the high concentration of $ONONO_2$.

Acknowledgements

The authors are grateful to Taiwan's National Center for High-performance Computing for the CPU, and Taiwan National Science Council for the research support to MCL for a Distinguished Visiting Professorship). RSZ thanks ONR for the support of this Letter at Emory University and KYL also acknowledges the help from Wen-Fei Huang and Shang-Ying Wu on rate constant prediction.

Appendix A. Supplementary data

Supplementary data associated with this article can be found, in the online version, at http://dx.doi.org/10.1016/j.cplett.2012.04.015.

References

[1] W. Tam, S. Wiley, K. Dommer, L. Mosher, D. Persons, Amer. Inst. Aeronaut. Astronaut. (2002) 4139.
[2] R.L. McNutt Jr., S.C. Solomon, R.E. Gold, J.C. Leary, the MESSENGER Team, Adv. Space Res. 38 (2006) 564.
[3] J.C. Leary et al., Space Sci. Rev. 131 (2007) 187.
[4] L.B. Zung, J.R. White, NASA Contractor Rep. (1971) 1704.
[5] L.E. Mosher, S. Wiley, John Hopkins APL Tech. Dig. 19 (2) (1998).
[6] S. Wiley, K. Dommer, L. Mosher, American Institute of Aeronautics and Astronautics/Society of Automotive Engineers/American Society of Mechanical Engineers Joint Propulsion Conference Paper AIAA-2003-5078, 2003, p. 20.
[7] H.G. Weiss, NASA Contractor Rep. (1965). 64338-06.
[8] M.C. Burrows, NASA Tech. Note (1968) D-4467.
[9] M. Herscb, NASA Tech. Note (1968) D-4776.
[10] B.P. Lawver, B.P. Breen, NASA Contractor Rep. (1968) 72444.
[11] D.A. Pinnick, S.F. Agnew, B.I. Swanson, J. Phys. Chem. 96 (1992) 7092.
[12] M.J. Frisch et al., Gaussian 03, Gaussian, Inc., Wallingford, CT, 2004.
[13] S.H. Vosko, L. Wilk, M. Nusair, Can. J. Phys. 58 (1980) 1200.
[14] C. Lee, W. Yang, R.G. Parr, Phys. Rev. B 37 (1988) 785.
[15] B. Miehlich, A. Savin, H. Stoll, H. Preuss, Chem. Phys. Lett. 157 (1989) 200.
[16] A.D. Becke, J. Chem. Phys. 98 (1993) 5648.
[17] C. Gonzalez, H.B. Schelgel, J. Chem. Phys. 90 (1988) 2154.
[18] A.M. Mebel, K. Morokuma, M.C. Lin, J. Chem. Phys. 103 (1995) 7414.
[19] S.J. Klippenstein, A.F. Wagner, R.C. Dunbar, D.M. Wardlaw, and S.H. Robertson, VARIFLEX: VERSION 1.00, 1999.
[20] G.M. Evans, M. Polanyi, Trans. Faraday Soc. 31 (1935) 875.
[21] H. Eyring, J. Chem. Phys. 3 (1935) 107.
[22] W.G. Fateley, H.A. Bent, B.J. Crawford, J. Chem. Phys. 31 (1959) 204.
[23] I.C. Hisatsune, J.P. Devlin, Y.J. Wada, J. Chem. Phys. 33 (1960) 714.
[24] R.V.S. Louis, B. Crawford Jr., J. Chem. Phys. 42 (1965) 857.
[25] E.L. Varetti, G.C. Pimental, J. Chem. Phys. 55 (1971) 3813.
[26] L. Parts, J.T. Miller, J. Chem. Phys. 43 (1965) 136.
[27] F. Bolduan, H. Jodl, Chem. Phys. Lett. 85 (1982) 283.
[28] F. Bolduan, H. Jodl, A. Loewenschuss, J. Chem. Phys. 80 (1984) 1739.
[29] S.F. Agnew, B.I. Swanson, L.H. Jones, R.L. Mills, D. Schiferl, J. Phys. Chem. 87 (1983) 5065.
[30] L.H. Jones, B.I. Swanson, S.F. Agnew, J. Phys. Chem. 82 (1985) 4389.
[31] A. Givan, A. Loewenschuss, J. Chem. Phys. 90 (1989) 6135.
[32] A. Givan, A. Loewenschuss, J. Chem. Phys. 91 (1989) 5126.
[33] A. Givan, A. Loewenschuss, J. Chem. Phys. 94 (1991) 7562.
[34] A. Stirling, I. Papai, J. Mink, D.R. Salahub, J. Chem. Phys. 100 (1994) 2910.
[35] M.L. McKee, J. Am. Chem. Soc. 117 (1995) 1629.
[36] I.I. Zakharov, A.I. Kolbasin, O.I. Zakharova, I.V. Kravchenko, V.I. Dyshlovoi, Theor. Exp. Chem. 44 (1) (2008).
[37] X. Wang, Q.-Z. Qin, K. Fan, J. Mol. Struct. (Theochem) 432 (1998) 55.
[38] I.C. Hisatsune, J. Phys. Chem. 65 (1961) 2249.
[39] T.J. Lee, J.E. Rice, G.E. Scuseria, H.F. Schaefer, Thcor. Chim. Acta 75 (1989) 81.
[40] T.J. Lee, P.R. Taylor, Int. J. Quantum Chem. S23 (1989) 199.
[41] P. Raghunath, private communication.